

<http://www.tandfonline.com/loi/gmcl19>

<sup>a</sup> Laboratoire de Physique des Solides Université Paris-Sud Centre Universitaire, Bât. 510, F-91405, ORSAY Cedex, France

Version of record first published: 04 Oct 2006

To link to this article: <http://dx.doi.org/10.1080/10587259708045093>

The publisher does not give any warranty express or implied or make any representation that the contents will be complete or accurate or up to date. The accuracy of any instructions, formulae, and drug doses should be independently verified with primary sources. The publisher shall not be liable for any loss, actions, claims, proceedings, demand, or costs or damages whatsoever or howsoever caused arising directly or indirectly in connection with or arising out of the use of this material.

# Dibenzotetraaza[14]Annulene Complexes. Part. 3:

## Mesomorphic Properties of Six and Eight Chain Substituted Compounds

S. FORGET and M. VEBER\*

*Laboratoire de Physique des Solides Université Paris-Sud Centre  
Universitaire, Bât. 510, F-91405 ORSAY Cedex, France*

*(Received 22 March 1997; Accepted 8 May 1997)*

The mesomorphic properties of some dibenzotetraaza[14]annulene complexes bearing six and eight alkoxy chains have been investigated by microscopic observations, DSC experiments and X-ray diffraction. In each case,  $D_h$  phases were identified. The influence of the number, the length and the position of the grafted chains on the liquid crystal behaviour is discussed.

**Keywords:** Metallomesogens; dibenzotetraaza[14]annulene; liquid crystals; X-ray studies

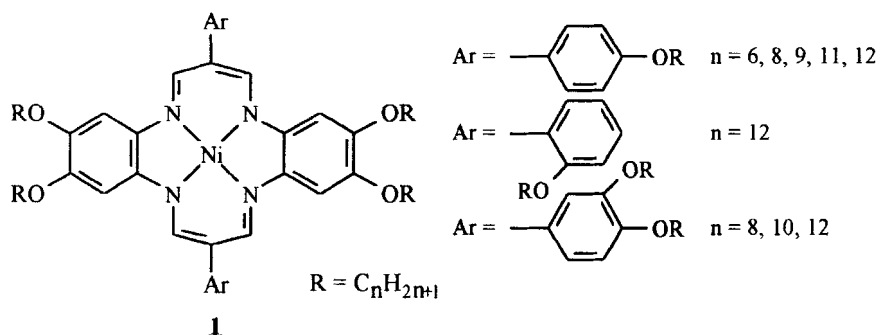
### INTRODUCTION

We have recently published the synthesis [1,2,3] and mesomorphic properties of four chain substituted dibenzotetraaza[14]annulene complexes and ligands. The influence of the chain length on the columnar hexagonal mesophase (transition temperatures and cell parameters) has been discussed. In order to have more insight into the mesomorphic properties and the molecular organization of the  $D_h$  mesophase, we have synthesized six and eight chain substituted derivatives varying the number and the position of the alkoxy chains.

---

\*e-mail: Veber @ ips. u-psvd. fr.

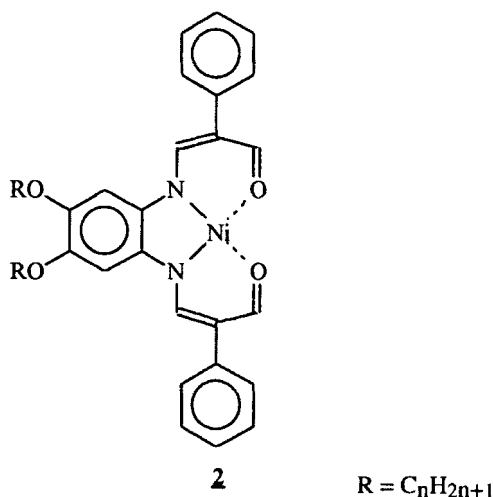
The general formula of the studied complexes is given below:



We used the following notation for these complexes: **XCn-z**, X representing the number of the paraffinic chains grafted on the macrocycle ( $X = 4, 6, 8$ ), **n**, the number of the carbon atoms per aliphatic chain ( $n = 6-12$ ), and **z** the position of the alkoxy chains on the aryl groups ( $z = o$  for ortho, **p** for para and **m** for meta); **z** is omitted for the four chain compounds [2].

The dibenzotetraaza[14]annulene complexes were obtained using a procedure already described [1, 2, 3]. The purity of the new complexes has been checked by IR,  $^1\text{H-NMR}$  and UV-visible spectroscopies [4].

Only symmetrical compounds have been synthesized. Yet, during the synthesis, an interesting intermediate has been isolated, namely the uncyclised complex **2** (identified by mass spectroscopy and  $^1\text{H-NMR}$  [5]):



This compound could lead to unsymmetric complexes by further condensation with different substituted orthophenylenediamines.

The mesomorphic properties of the whole series were studied by microscopic observations under polarized light, and by DSC and X-Ray diffraction. They are presented below.

### 1. Microscopic Observations

Microscopic observations were performed with a Leitz Orthoplan polarized microscope equipped with a Mettler FP5 variable temperature stage. Transition temperatures and enthalpies were determined with a DSC7 Perkin Elmer apparatus.

The microscopic study has shown for compounds **6Cn-p** total decomposition of the sample if  $n < 10$  and partial decomposition if  $n \geq 10$  when reaching the clearing temperature (the decomposition has been checked by TLC). To avoid the perturbations due to some decomposition of the samples during the DSC measurements, each experiment was performed without reaching the clearing temperature. This enabled reproducible temperature cycles to be obtained (as already described [2]).

In the same way, typical textures have been grown either by cooling from the isotropic phase or by slow evaporation of a solvent (dichloromethane or toluene) to avoid decomposition of the samples as described in references 1 and 2.

Compounds **6Cn-p** and **8Cn-mp** present the same mesomorphic behaviour. When heating, there is a transition to a red viscous birefringent phase, different from the original crystalline one. Upon cooling, this phase remains down to room temperature. No decomposition has been detected for the **8Cn-mp** compounds before clearing.

The textures obtained are presented on Figure 1. We can see the dendritic growth of monodomains, linear defects (Plate 1, compound **6C11-p**) as well as the growth of some hexagons from the isotropic phase (Plate 2, compound **6C6-p**) due to the slow evaporation of the solvent. Fan-shaped textures appear on the top of some hexagons. We can notice that these hexagons show very sharp edges. In some cases, by slow evaporation of toluene, some six dendritic domains appear (Plate 3, compound **6C8-p**). All these textures are characteristic of columnar hexagonal phases  $D_h$  [6].

The compound **6C12-o**, in which the aryl groups are substituted by a dodecyloxy group grafted at the ortho positions, shows completely different behaviour: it seems to be crystalline and melts only into an isotropic liquid phase.



**Plate 1** : Compound **6C11-p**,  $T=325^{\circ}\text{C}$

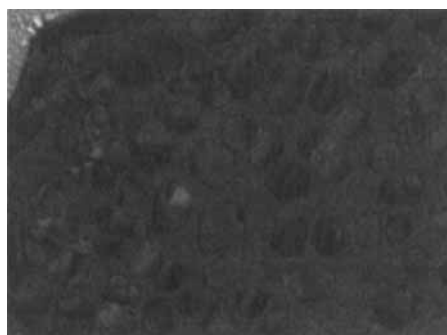


**Plate2** : Compound **6C6-p**,  $T=95^{\circ}\text{C}$



**Plate 3** : Compound **6C8-p** (toluene),  $T=90^{\circ}\text{C}$

FIGURE 1 Textures exhibited by some **6Cn-p** complexes. (See Color Plate I).

## 2. DSC

All the complexes **6Cn-p** and **8Cn-mp** have been studied by DSC. The results are summarized in Table I.

Typical curves were given in reference 1 for the **6C12p** and **8C12-mp** complexes. On each **6Cn-p** and **8Cn-mp** thermogram, upon heating, a transition towards a phase, different from the crystalline one, is detected (complex **6C12-p**:  $T = 24^\circ\text{C}$ ,  $\Delta H = 27.4 \text{ J}\cdot\text{g}^{-1}$  and complex **8C12-mp**:  $T = 18^\circ\text{C}$ ,  $\Delta H = 13.3 \text{ J}\cdot\text{g}^{-1}$ ). Upon cooling the corresponding recrystallisation

TABLE I Transition temperatures, enthalpies, cell parameters of the hexagonal lattice and number of molecules per unit cell of the dibenzotetraaza[14]annulene **XCn-z** complexes

Compound	<i>a</i> ( $\text{\AA}$ )	<i>c</i> ( $\text{\AA}$ )	<i>n<sub>c</sub></i>	Transition temperatures ( $^\circ\text{C}$ ) (Transition enthalpies ( $\text{J/g}$ ))
<b>6C6-p</b>	24.6	3.36	0.96	Cr $\xrightleftharpoons[25.2(5.4)]{40.8(5.4)}$ D <sub>h</sub> $\xrightarrow{> 300}$ I*
<b>6C8-p</b>	26.6	3.36	0.98	Cr <sub>1</sub> $\xrightarrow{12.3(2.5)}$ Cr <sub>2</sub> $\xrightarrow{25.6(0.1)}$ D <sub>h</sub> $\xrightarrow{369.7}$ I* $\xleftarrow{-0.3(2.1)}$
<b>6C9-p</b>	27.6	3.36	0.99	Cr <sub>1</sub> $\xrightarrow{15.6(5.7)}$ Cr <sub>2</sub> $\xrightarrow{23.6(0.1)}$ D <sub>h</sub> $\xrightarrow{360}$ I* $\xleftarrow{4.6(5.4)}$
<b>6C11-p</b>	29.9	3.38	1.04	Cr <sub>1</sub> $\xrightleftharpoons[3.3(-17.9)]{-9.6(0.4)}$ Cr <sub>2</sub> $\xrightleftharpoons[23.8(0.1)]{11.5(2)}$ Cr <sub>3</sub> $\xrightarrow{16.6(12)}$ D <sub>h</sub> $\xrightarrow{337}$ I* $\xleftarrow{23.8(0.1)}$
<b>6C12-p</b>	31.4	3.39	1.09	Cr $\xrightleftharpoons[16(27.4)]{24(27.4)}$ D <sub>h</sub> $\xrightarrow{> 300}$ I*
<b>6C12-o</b>				Cr $\xrightleftharpoons[27.65(4.3)]{31.1(3.6)}$ Cr $\xrightleftharpoons[92.8(66.9)]{122.3(66.5)}$ I
<b>8C8-mp</b>	29.1	3.35	0.97	
<b>8C10-mp</b>	31.45	3.34	0.98	Cr $\xrightleftharpoons[-21.1(8.2)]{-12(9.1)}$ D <sub>h</sub> $\xrightleftharpoons{260.1}$ I
<b>8C12-mp</b>	—	—	—	Cr $\xrightleftharpoons[11(13)]{18(13.3)}$ D <sub>h</sub> $\xrightleftharpoons{250}$ I

\*Partial or total decomposition of the sample, checked by TLC.

appears at lower temperature ( $\Delta T = 7-8^\circ\text{C}$ ). In any case, the samples were heated only to  $200^\circ\text{C}$ . Under these conditions, the thermograms were reproducible.

No transition was detected by DSC in the range  $-70^\circ\text{C}$  to  $200^\circ\text{C}$  for the compound **8C8-mp** (the sensitivity of the DSC apparatus was less than  $0.1\text{ J}\cdot\text{g}^{-1}$ ). But its X-ray pattern allowed us to identify a  $D_h$  mesophase at room temperature as described in the following paragraph.

The phase sequence displayed by the compound **6C12-o** is given in Figure 2 and summarized below:

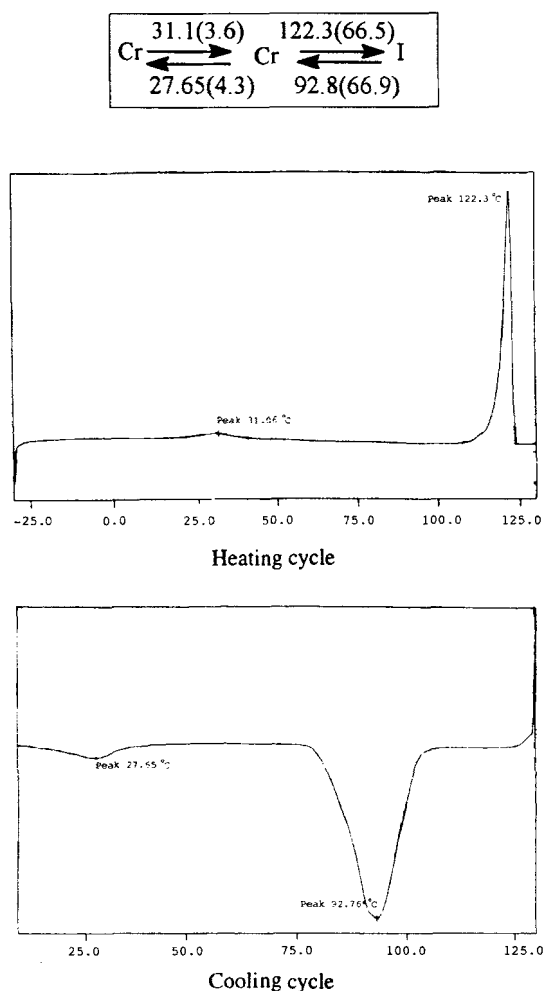


FIGURE 2 Thermogram of the **6C12-o** complex.

Two transitions are detected upon heating, the first one, of low enthalpy, corresponds to a crystal–crystal transition and the second one, of high enthalpy, is the transition from the second crystalline phase to the isotropic phase. Some supercooling (29.5°C) is observed by lowering the temperature from the isotropic phase to the Cr<sub>2</sub> phase. The transition from this phase to the Cr<sub>1</sub> phase is observed at 27.7°C. The high value of the melting and recrystallization transition enthalpies supports assignment of **6C12-o** as non-mesomorphic.

All the synthesized complexes **6Cn-p** and **8Cn-mp** which seem to display some mesomorphic behaviour by microscopy and DSC have been studied by X-Ray diffraction.

### 3. X-Rays Diffraction Studies

Aligned sample (**6C12-p**) were obtained by shearing a small droplet of product on a thin mica crystal sheet with a smooth spatula, as already described [2]. Patterns were obtained using setups already described [2, 7]. A Guinier powder camera was used to measure accurately the structural parameters of the mesophase [8].

Figure 3a presents a typical example of **XCn-z**'s powder pattern (compound **6C12-p**). At wide angles, a weak diffuse peak can be detected around  $s = 1/4 \cdot 5 \text{ \AA}^{-1}$  ( $s$  is the scattering vector), corresponding to interference from the disordered parts of the molecules, the melted paraffinic chains, characteristic of mesomorphic compounds. At wide angles another peak, less diffuse, can be seen, due to core–core interactions. It characterizes the stacking of the molecules inside the columns. At small angles the observed peaks are characteristic of a two-dimensional hexagonal lattice: the corresponding lattice spacings are in ratios  $1:\sqrt{3}:2:\sqrt{7}$ .

All the studied compounds (**6Cn-p** and **8Cn-mp**) show, in the temperature range determined by the DSC measurements, a D<sub>h</sub> phase identified by X-Ray experiments (powder samples pattern) in agreement with the microscopic observations.

Even in the case of the **8C8-mp** complex, for which no transition peaks were detected by DSC, a D<sub>h</sub> mesophase was identified by X-Rays experiments. The powder pattern of this **8C8-mp** complex is given in Figure 4. The different cell parameters are presented in Table I as well as the number of molecules per unit cell ( $n_c$ ), determined according to [2]:

$$\rho = n_c M / NV$$



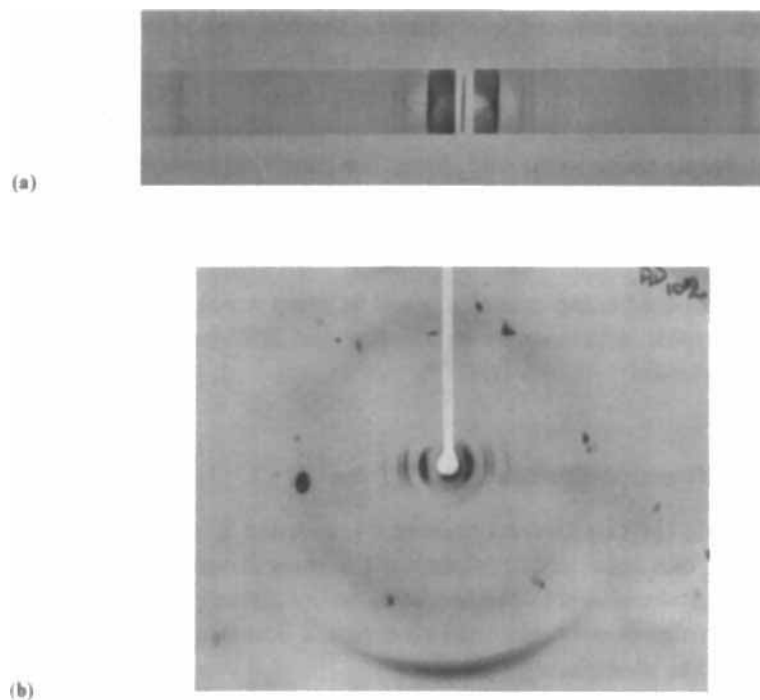


FIGURE 3 a/ Powder pattern of the **6C12-p** complex, b/ Aligned pattern of the **6C12-p** complex.

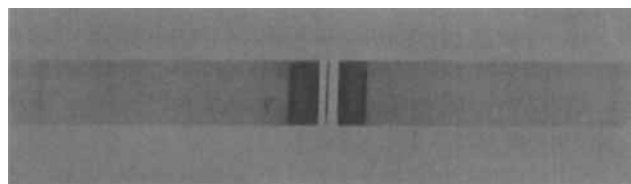


FIGURE 4 Powder pattern of the **8C8-mp** complex.

where  $n_c$  corresponds to the number of molecules per unit cell;  $\rho$ , to the molecular density.  $N$ , is the Avogadro number;  $V$ , the unit cell volume ( $V = (\sqrt{3}/2)a^2c$ ),  $M$ , the molecular mass. In all the cases, the density,  $\rho$ , of the mesophase was assumed to be close to one.

The X-ray diffraction pattern of an aligned sample of complex **6C12-p** has been measured and is presented on Figure 3b. Some small angle reflections, located along the equator, are detected in a spacing ratio  $1, \sqrt{3}, 2, \sqrt{7}, 3$ .

These reflection peaks characterize the two-dimensional lattice: a hexagonal one in the plane of the molecules. An outer reflection (diffuse crescent) is oriented along the meridian, along the spreading direction. This diffusion is due to some core–core interactions along the column axis. It confirms that the two-dimensional lattice is perpendicular to the spreading direction and that the columns are oriented along this direction.

From the width of the wide angle reflection on the aligned pattern, the intracolumnar correlation length,  $L_p$  can be deduced. This length, corresponding to the average size of columns where some core–core interactions exist, is related to the number of stacked molecules. For **6C12-p** complex, we calculated  $L_p = 167 \text{ \AA}$  corresponding to approximately 50 molecules. This value is the same as in the case of the previously described **4Cn** complexes [2], where 45 to 50 molecules were found regularly stacked.

#### 4. Discussion

The influence of the chain length and the number of grafted chains on the transition temperatures deduced from the data of Table I is collected in Figure 5 where transition temperatures for each series versus the chain length  $n$  are plotted. The results of the four chain derivatives are also reproduced [2].

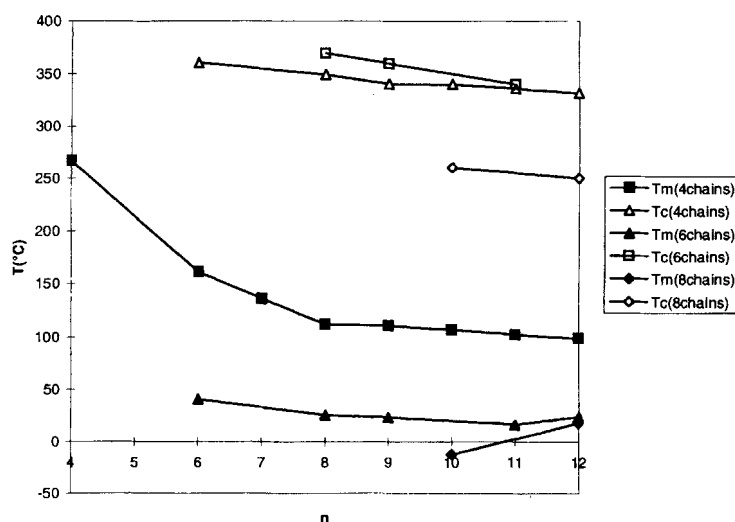


FIGURE 5 Melting and clearing temperatures of the **XCn-z** complexes as a function of chain length.

The mesomorphic behaviour appears at room temperature, or even below for the **8Cn-mp** compounds, and persists over a wide temperature range ( $\approx 300^\circ\text{C}$ ).

As expected, as the chain length increases, the clearing temperatures decrease. This can be seen with the eight chain **8Cn-mp** compounds:  $T_c(n=10) = 260.1^\circ\text{C}$  and  $T_c(n=12) = 250^\circ\text{C}$ . In the case of the six chain compounds, the clearing temperatures are in fact temperatures of partial decomposition. As the number of chains increases, the melting temperatures decrease greatly from the four to six chain derivatives and even more for the eight chain ones, as do the clearing temperatures. No odd-even effect is observed for **6Cn-p** complexes,  $n = 6, 8, 9, 11, 12$ .

We have still noticed that dibenzotetraaza[14]annulene derivatives have a tendency to decompose when heated to high temperature ( $> 300^\circ\text{C}$ ), particularly in the case of the four [2] and six chain compounds. By decreasing the clearing temperature (namely by adding chains), the complexes are stable enough to undergo transition into the isotropic phase without decomposing. Indeed, this is the case of the **8Cn-mp** compounds (the purity of the samples has been checked by TLC before and after heating).

As all the compounds display the same  $D_h$  mesophases, it is interesting to compare the geometric parameters of these phases for all the compounds of the series, namely the hexagonal parameter, **a** and the stacking periodicity, **c**. This is presented in Figure 6.

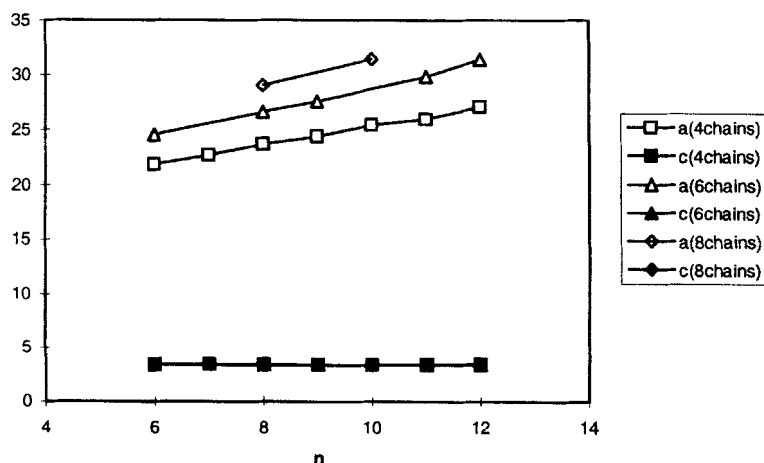


FIGURE 6 Variations of the parameters **a** and **c** with the chain length.

We can see that in a given series the hexagonal lattice parameter,  $a$ , regularly increases with  $n$ , whereas there is no noticeable change in the  $c$  parameter. This means that the chain length seems to have no influence upon the mesomorphic phase organization of the dibenzotetraaza[14]annulene derivatives.

When the number of chains increases, we observe an expected increase in the hexagonal  $a$  parameter. On the other hand, the number of chains seems to have no influence on the  $c$  parameter ( $c \approx 3.36 \text{ \AA}$ ) whatever the number (4, 6 or 8) and the length ( $n$ ) of the paraffinic chains. It can be noticed that such values are among the shortest encountered in columnar hexagonal phases [7] and might be the sign of strong  $\pi-\pi$  interactions inside the columns.

From the parameters  $a$  and  $c$  we can deduce the unit cell volume (according to  $V = (\sqrt{3}/2)a^2c$ ). In Figure 7 is plotted this hexagonal cell volume versus the total number of carbon atoms in the aliphatic chains. Within experimental error, all points fall on a straight line. The slope of this straight line gives the mean volume per methylene group,  $V_m = 28 \text{ \AA}^3$ . This volume is a classical value compared to what is usually found for other discotic compounds [5]. Moreover, the intercept of this straight line is

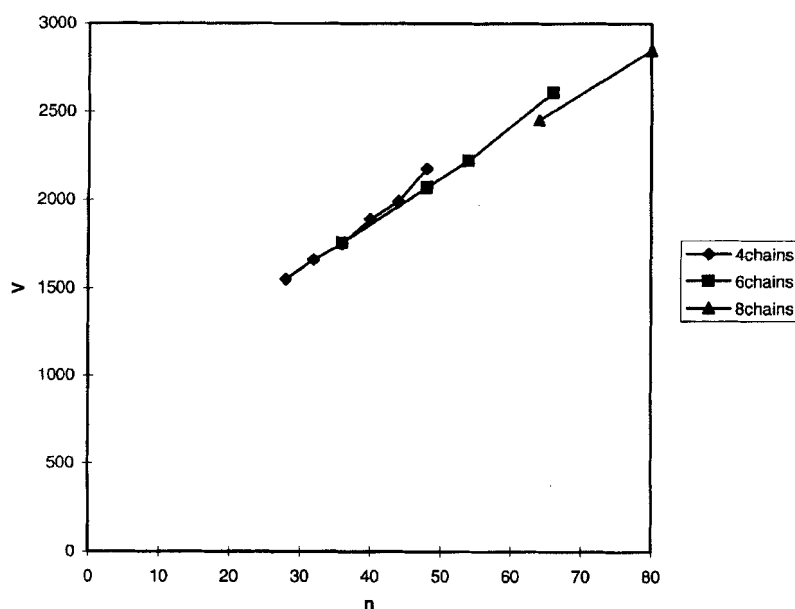


FIGURE 7 Volume of the unit cells as a function of the total number of carbon atoms of the  $\text{XCn-z}$  complexes.

associated to the apparent volume of the non aliphatic part of the compounds ( $750 \text{ \AA}^3$ ) from which we can deduce the apparent core radius:  $R = 8.1 \text{ \AA}$ . Those results are in agreement with the distances measured on a molecular model (Hyper Chem modelling software [2]) in which we obtained two characteristic core radii:  $R_{\text{max}} = 8.6 \text{ \AA}$  and  $R_{\text{min}} = 5.7 \text{ \AA}$ . (**6C1-p** complex). The apparent core value is very close to  $R_{\text{max}}$ .

From the apparent core radius  $R$ , we can deduce the apparent length of the paraffinic chains  $l$ . This value is compared to the length of a paraffinic chain in an all trans conformation  $L$ . We have plotted the ratio  $x$  ( $x = L/l$ ) versus the chain length for each compound of the studied series,  $x$  characterises the order in the organization of the paraffinic chains. This was done for all the studied complexes and is given in Figure 8. Within a series there are very few variations. The chains in the compounds **4Cn** appear very mobile and disorganized (high  $x$  values). When the number of chains increases, the chains become more organized and come up to the case of all trans crystallised chains, this is the case for the **8Cn-mp** complexes ( $x$  values close to one).

Since the mesophase displayed by all the compounds seems not only to be of the same symmetry ( $D_h$ ) but also to present the same type of packing, we tried to model the molecular organization of this  $D_h$  phase. Taking into account the former results, this model might be valid for all the **XCn-z** complexes. Moreover, it would give access to the apparent aromatic core

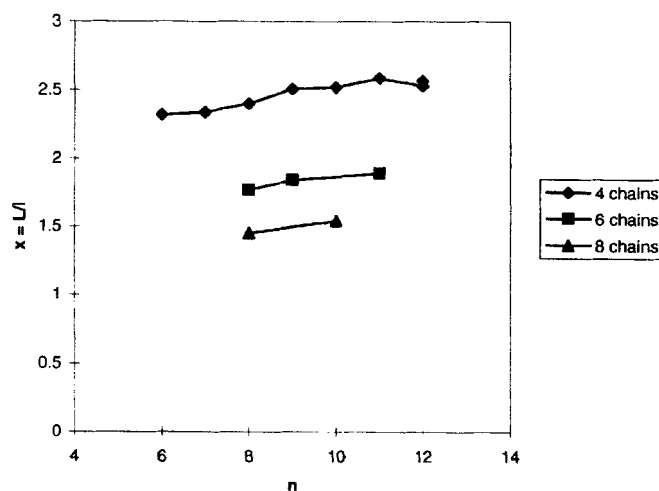


FIGURE 8 Bending state ( $L/l$  ratio) of the chains in the **XCn-z** complexes as a function of the chain length.

radius that would be compared to the radius deduced from the cell volume.

Such a model may be derived by evaluating the intensity distribution of the different 2D lattice reflections for each compound. Table II shows the qualitative evaluation of the reflections intensities for all the members of the homologous series. These intensities have been directly estimated from powder patterns and corrected for the Lorentz–polarization and multiplicity factors [7].

One can notice that as the chain length decreases within a series, the extinction moves towards higher interreticular distances (higher order) except for the compounds **4C6**, **6C6-p** and **8Cn-mp**, for which an intensity inversion occurs between the reflections (20) and (21). The case of the compounds **4C9** and **6C6-p** is interesting as both have 36 methylene groups in the aliphatic chains. They show different intensity profiles: contrary to what we had firstly thought, the molecular organization is different from one series to another, depending on the number of grafted chains on the dibenzotetraaza[14]annulene core. So each series must be considered independently.

A very simple model is a two component system where the molecules are divided into two concentric cylindrical domains. The outer domain is of low and uniform density which has been taken equal to zero ( $\rho = 0$ ). The central

TABLE II Intensities of the different 2D lattice reflections directly estimated on powder patterns of nickel complexes **4Cn**, **6Cn-p** and **8Cn-mp**, and corrected for the Lorentz–polarization and multiplicity factors (VS: very strong; S: strong; m: medium; w: weak; vw: very weak;----: not observed), deduced radius  $R'$

	$n$		$(hk)$					$R'(\text{\AA})$
			(10)	(11)	(20)(02)	(21)	(30)	
<b>4Cn</b>	12	VS	S	w	vw	–	–	11.1
	11	VS	m	w	vw	–	–	10.6
	10	VS	m	w	vw	–	–	10.3
	9	VS	S	m	w	vw	–	10.1
	8	VS	w	vw	vw	–	–	9.8
	7	VS	S	m	m	vw	–	9.5
	6	VS	w	vw	w	vw	–	9.7
<b>6Cn-p</b>	12	S	m	w	vw	–	–	13
	11	VS	S	w	vw	–	–	12.5
	9	VS	S	w	w	–	–	11.7
	8	VS	m	w	w	–	–	11.2
	6	VS	m	w	m	vw	–	10.6
<b>8Cn-mp</b>	10	VS	S	vw	w	–	–	7.6
	8	VS	w	vw	w	–	–	7.6

one is of larger and uniform electronic density and has been taken equal to 1 ( $\rho = 1$ ).

If we suppose that the columns are located at the edges of the hexagonal lattice (on the  $C_6$  axis), the intensity becomes:

$$F(s) = 2\pi \int_0^R J_0(2\pi rs) dr \text{ and } I(s) = K \frac{J_1^2(2\pi R's)}{s^2}$$

where  $K$ : constant factor,  $s$ : wave vector,  $J_0$ : Bessel function of zero order.

It implies a lot of intensity inversions. For each compound, i.e. for a given interreticular distance, we choose the core radius that gives the closest calculated intensity distribution given in Table II. The different values ( $R'$ ) are also listed in this table. This apparent core radius  $R'$ , related to the zone of greatest electron density, is different from one series to another. Nevertheless, in the case of the eight chain compounds (**8Cn-mp**), the calculated radius ( $R' = 7.6 \text{ \AA}$ ) can be compared with the radius deduced from the X-ray study ( $R = 8.1 \text{ \AA}$ ) and with the two radii measured on the stereomodel ( $R_{\min} = 5.7 \text{ \AA}$  and  $R_{\max} = 8.6 \text{ \AA}$ ). We can notice that the value obtained is located between  $R_{\min}$  and  $R_{\max}$  (closer to  $R_{\max}$ ). It means that most of the aromatic area belongs to the organized part of the molecule.

Moreover, in the case of the four and six chain compounds, the apparent core radius  $R'$  is different from one compound to another, in the same series. So we can conclude that this simple model (one box) is not representative of the molecular organization inside the columnar mesophase, even if we consider a very small core of high electronic density (the metal). The principle of the two component model implies that the central cylindrical box has a rough and well defined frontier area. This is not true in the case of the four chain compounds in which the rectangular shape of the core seems to have some influence: it might be responsible for a modulation (smoothness) of the interface between the two media of different density.

## CONCLUSION

We have shown that the dibenzotetraaza[14]annulene derivatives have a great tendency to self-organize in columns and form columnar hexagonal phases. Whatever the number (4, 6 or 8) of chains and their length ( $n \geq 6$ ), they display these columnar hexagonal mesophases over a very wide range of temperature. Moreover, the mesophase exists from room temperature for most of them. The columnar phase has been studied by DSC, microscopic

observations and X-rays measurements. The volume per methylene group, the apparent volume of the unit cells and the number of molecules per cell were determined. As for the four chain substituted compounds previously reported [2], the different results imply that there are strong  $\pi$ - $\pi$  interactions within the columns (short *c* distances).

In order to disturb this organization, a compound with ortho substituents has been synthesized. Such substituents inhibit core-core interactions: the transition temperature towards the isotropic phase is greatly lowered but the compound is no longer a liquid crystal.

We have discussed the molecular organization inside the mesophase and deduced the apparent volume of the non disorganized part of the molecules. This core volume is valid for each of the derivatives studied. We have also tried to model the molecular organization with a simple two component system model. This is appropriate for the **8Cn-mp** complexes, leading to a radius of high electronic density area close to the calculated (or measured) radii. Nevertheless, in the case of the **6Cn-p** and **4Cn** complexes, such a model fails. The columns can no longer be viewed as well defined cylinders of high electronic density surrounded by a dense crown of paraffinic chains. Work is in progress in order to obtain more insight into the molecular organization inside the columns in such peculiar cases.

## References

- [1] S. Forget, M. Veber and H. Strzelecka, *Mol. Cryst. Liq. Cryst.*, **258**, 263–275 (1995).
- [2] S. Forget, M. Veber and A. M. Levelut, *Mol. Cryst. Liq. Cryst.*, in press (1997).
- [3] S. Forget and M. Veber, *New J. Chem.*, **21**, 409–411 (1997).
- [4] Typical spectra:
  - 6C12-p:** UV  $\lambda(\text{nm})(\log \epsilon)$ : 530(3.88); 462(4.83); 314(4.73).  
 IR  $\nu(\text{cm}^{-1})$ ; KBr Pellets:  $\nu(\text{CH}_2)$  2929;  $\nu(\text{CH}_2)$  2849;  $\nu(\text{N}=\text{C}-\text{C}=\text{N})$  1607;  $\nu(\Phi_{\text{OR}})$  1269;  $\nu(\Phi_{\text{OR}})$  1015.  
 NMR ( $\text{CDCl}_3$ ): 0.85 (t, 18H,  $\text{CH}_3$ ); 1.25, 1.5, 1.7 (m, 120H,  $\text{CH}_2$ ); 3.75 (t, 8H,  $\text{OCH}_2$  dibenzo); 3.9 (t, 4H,  $\text{OCH}_2\text{Ar}$ ); 6.8 (s, 4H, H dibenzo); 7.05 (A-B syst., 8H, Ar); 7.2 (s, 4H, 5, 7, 12, 14-H).
  - 6C12-o:** UV  $\lambda(\text{nm})(\log \epsilon)$ : 515.5(3.88); 455(4.92); 325(4.73).  
 NMR ( $\text{CDCl}_3$ ): 0.85 (t, 18H,  $\text{CH}_3$ ); 1.25, 1.75 (m, 120H,  $\text{CH}_2$ ); 3.8 (t, 8H,  $\text{OCH}_2$  dibenzo); 4.0 (t, 4H,  $\text{OCH}_2\text{Ar}$ ); 6.5–8.0 (broad m, 8H, aromatic H).
  - 8C12-mp:** UV  $\lambda(\text{nm})(\log \epsilon)$ : 532(4.00); 462(4.92); 316(4.83).  
 IR  $\nu(\text{cm}^{-1})$ ; KBr Pellets:  $\nu(\text{CH}_2)$  2922;  $\nu(\text{CH}_2)$  2850;  $\nu(\text{N}=\text{C}-\text{C}=\text{N})$  1604;  $\nu(\Phi_{\text{OR}})$  1266.  
 NMR ( $\text{CDCl}_3$ ): 0.9(t, 24H,  $\text{CH}_3$ ); 1.35, 1.47, 1.8(m, 160H,  $\text{CH}_2$ ); 4.0(m, 16H,  $\text{OCH}_2$ ); 6.8(s, 4H, H dibenzo); 6.85 (m, 6H, Ar); 7.4(s, 4H, 5, 7, 12, 14-H).
- [5] Mass spectrum:  $M + 1 = 737 \text{ g.mol}^{-1}$ .  
 $^1\text{H-NMR}$ : d(ppm): 0.9 (t, 6H,  $\text{CH}_3$ ), 1.3 (m,  $\text{CH}_2$ ), 1.8 (m, 4H,  $\text{O-CH}_2\text{-CH}_2$ ), 3.9 (t, 4H,  $\text{O-CH}_2$ ), 6.9 (s, 2H, aromatic from orthophenylene), 7.25–7.35 (m, 10H, aromatic of the aryl groups), 7.6 (d, 4H, ethylenic).



- [6] a) P. Oswald, *J. Phys. France*, **49**, 1083–1089 (1988).  
b) P. Oswald, *J. Phys. France*, **49**, 2119–2124 (1988).
- [7] M. Veber, P. Sotta, P. Davidson, A. M. Levelut, C. Jauabert and H. Strzelecka, *J. Phys. France*, **51**, 1283 (1990).
- [8] A. Guinier, “Théorie et technique de la radiocristallographie”, Dunod Paris, 1956.